IMPROVED NAKAGAMI IMAGING USING A COMBINED ESTIMATOR

A. Larrue, J.A. Noble

Institute of Biomedical Engineering
Department of Engineering Science
University of Oxford, Oxford OX3 7DQ, UK

ABSTRACT

Nakagami imaging is an ultrasonic tissue characterization technique which has shown promise for differentiating different breast masses. Two parameters describing the shape and the scale of the distribution of the RF-data envelope can be computed using sliding windows. Though the traditional moment-based estimator is theoretically unbiased, its performance is not stable and depends on the value of the parameters. In this work, we propose a framework combining two estimators to improve and homogenize the accuracy of the estimation. This is done by computing both parameters and deciding *a posteriori* which is the best by measuring the goodness of fitting between the estimated theoretical distribution and the observed one. We test this method both on synthetic images presenting real US speckle pattern structures and a Nakagami distribution with chosen parameters and on clinical US breasts images. Results show a considerable improvement of the accuracy and of the stability of the estimations over conventional estimation.

Index Terms— Ultrasound tissue characterization, Nakagami Imaging

1. INTRODUCTION

The possibility of characterizing tissues with ultrasound (US) has been well-established. As the quality of the US RF-signals has increased in the last years, US tissue characterization has become an important area of research. Differences in the tissue microstructure lead to differences in the scattering patterns that can be measured by computing parameters from the ultrasonic backscattered signal. In [1], Shankar proposed to model the distribution of the values of the log-compressed envelope of the US signal with a Nakagami distribution. The Nakagami family of distributions is defined as:

$$f(r) = \frac{2m^m r^{2m-1}}{\Gamma(m)\Omega^m} e^{-\frac{m}{\Omega}r^2} \quad , \; r > 0 \qquad (1)$$

where r is the log-compressed envelope of the signal, Ω is a scale parameter related to the local backscattered energy and m describes the shape of the distribution. This describes all backscattering conditions met in medical ultrasound, including Rayleigh ($0.5<m<1$), pre-Rayleigh ($m<0.5$) and post-Rayleigh ($m>1$). Nakagami imaging consists of computing the m and Ω parameters from the distribution of the values included in a *sliding window* spanning the whole image. It has been demonstrated that Nakagami imaging enables the estimation of the local concentration of scatterers in tissue, as it is correlated with the shape (m) parameter [2]. Medical applications using Nakagami Imaging to classify tumors are currently being developed[3].

Generally, the parameters are estimated using the 2nd and 4th order moments of the distribution. A well known issue addressed in [4] is the choice of the size of the window. Although a large number of points is needed for the estimation to be stable, large windows may contain more than one type of tissue. In the estimation of Ω, the utilization of large windows only affects the spatial resolution of the corresponding parametric image. As the estimation of m is very sensitive, estimation made by large and small windows is poor. Other subjects of investigation include the characteristics of the transducer [5]. Although the traditional estimator (i.e used in [2]) is theoretically unbiased, experiments show its performance depends on the values of m and Ω.

In this paper, we propose a new framework that considers multiple estimators in order to improve and homogenize the accuracy of the estimation. In addition to the traditional estimator, we propose to compute a maximum-likelihood (ML) based estimation [6] of the parameters. The best set of parameters is chosen by measuring the goodness of fitting between the estimated theoretical distributions (one for each pair of parameters) and the observed one.

First, we define the traditional, ML-based estimator and the chosen measure of the goodness of fitting, and then describe the new framework. Then we propose a novel method to create synthetic images presenting real US speckle pattern structures and a Nakagami distribution with chosen parameters. This enables us to test the performance of our method and to highlight the failure of the traditional one. Finally, we exemplify the new method with clinical breast images and quantify its benefits.

2. METHOD

2.1. Mathematical tools

For a given signal *r* whose values follow a Nakagami distribution, the parameters are traditionally estimated by the moment-based (MB) method using:

$$\Omega = \mathrm{E}(\mathrm{r}^2) \text{ and } \mathrm{m_a} = \frac{[\mathrm{E}(\mathrm{r}^2)]^2}{\mathrm{E}[\mathrm{r}^2 - \mathrm{E}(\mathrm{r}^2)]^2} = \frac{[\mathrm{E}(\mathrm{r}^2)]^2}{\mathrm{E}(\mathrm{r}^4) - [\mathrm{E}(\mathrm{r}^2)]^2} \quad .$$

A second method [6] uses a maximum-likelihood (ML) estimation which can be considered as an approximation of a minimum variance unbiased (MVU) estimator. In practice, it can be expressed as:

$$\mathrm{m_b} = \frac{6+\sqrt{36+48\Delta}}{24\Delta} \quad ;$$

Where:

$$\Delta = ln\left[\frac{1}{N}\sum_{i=1}^{N} r^2\right] - \frac{1}{N}\sum_{i=1}^{N} ln(r^2) = ln(\Omega) - E[ln(r^2)]$$

This second estimator was chosen in our work for the simplicity of its implementation, whilst it has shown good performance [6].

In order to measure *a posteriori* the goodness of fitting of the model regarding the observed data, we use the Kolmogorov-Smirnof (KS) distance :

$$d_{KS} = max_r\left(\left|F(r) - \hat{F}(r)\right|\right)$$

where F and $\hat{F}$ are respectively the cumulative distribution function (CDF) of the observed data and of the Nakagami distribution whose parameters are the ones estimated by one of the two methods above.

2.2. Implementation

To form the Nakagami images, the two parameters are estimated at each point from the values within a window of fixed size around it. The choice of the size of the windows is a critical parameter which is discussed in [2]. In this work, the size has been empirically chosen as ~2x2mm (161 pxl).

In our framework, for each pixel, two sets of parameters are estimated for each of the two methods described above. For each pair, the corresponding theoretical Nakagami distribution, its CDF, and the CDF of the observed distribution are calculated. The computation of the KS-distance between the two CDFs is then straightforward. The Nakagami image values at this pixel take then the values of the parameters with the smallest distance. For practical reasons, the computations are done with binned values, which leads to compute the 2nd and 4th order moments from the local histograms (10^4 bins). As the dynamic range of US images is known to be exponential, a logarithmic scale was used, which proved experimentally to lead to better estimations (cf. Results).

2.3. Generating Nakagami synthetic images

For the test and validation of our method, synthetic images presenting Nakagami distributions of known and fixed parameters must be used. Images of physical phantom or simulations are not suitable as they are time-consuming to create (of the order of hours), while the exact setting of the Nakagami parameters is difficult. By contrast, it is fast and easy to generate random samples from a defined Nakagami distribution. However, the structure of speckle which is known to be of great importance in US image analysis is lost. To overcome this problem, we propose to rearrange generated values of Nakagami distributions following the geometrical structure of the speckle extracted from a real US image.

First, a despeckling filter [7] is applied to a region of interest (ROI) of a real US image presenting a classical regular speckle pattern (Fig.1.a), so that the speckle can be extracted by subtraction (Fig.1.b). As the filter is not perfect, some regions show "flat" speckles. The contrast of the image is standardized using

$$\widetilde{Sp}(x,y) = \frac{Sp(x,y) - D_{10\%}(W_{x,y})}{D_{90\%}(W_{x,y}) - D_{10\%}(W_{x,y})} \quad ,$$

where Sp is the extracted speckle image, and $D_{10\%}(W_{x,y})$ and $D_{90\%}(W_{x,y})$ are respectively the 1st and 9th deciles of the values in the window $W_{x,y}$ around the point (x,y). $\widetilde{Sp}$ (Fig. 1.c) is the uniform speckle image which represents the geometrical structure of the speckle. For any given parameter pair (Ω,m), a random variable of the corresponding Nakagami distribution can be computed from Gamma random variable generator using the equivalence Nakagami(Ω,m)=Gamma(Ω,m/Ω). Finally, the generated random samples are arranged to adopt the structure of the speckle pattern. This can be done by sorting each set of values and associating the values of same rank. The Nakagami synthetic image NSI is defined as:

$$\mathrm{NSI}(\mathrm{x},\mathrm{y}) = \{\mathrm{Nakagami}(\Omega, m)\}^{\mathrm{s}}{}_{\mathrm{n}}$$

Where $\{\mathrm{Naka}(\Omega, m)\}^{\mathrm{s}}{}_{\mathrm{n}}$ is the n^{th} element of the sorted set of N generated values $\{\mathrm{Naka}(\Omega, m)\}^{\mathrm{s}}$, N being the number of pixel in the image, and n chosen so that:

$$\widetilde{Sp}(x,y) = \left\{\widetilde{Sp}\right\}^{\mathrm{s}}{}_{\mathrm{n}} ,$$

where $\left\{\widetilde{Sp}\right\}^{\mathrm{s}}{}_{\mathrm{n}}$ is the n^{th} element of the sorted set of values of the pixels of $\widetilde{Sp}$.

Fig. 1.e and 1.f show typical synthetic images for m=0.7/Ω=0.1 and m=0.3/Ω=0.1. Using this method, one can be sure that the distribution of the values follows a

Nakagami distribution of given parameters, whilst the structure of the speckle is respected. Though further testing could be done, we did not notice any local concentration of the lowest or highest values thanks to the local standardization of the contrast.

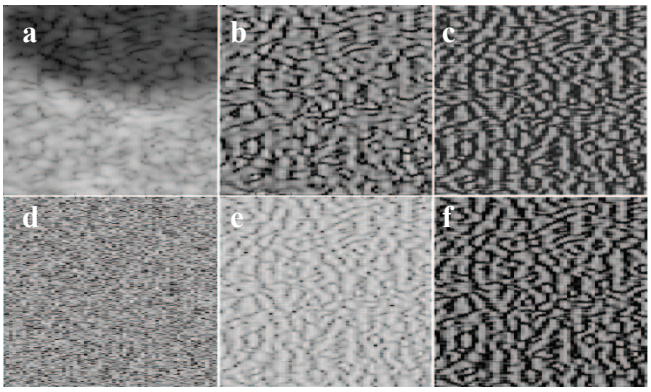


Figure 1: Formation of a synthetic image. a: original image (ROI), b: after speckle extraction, c: Speckle structure, d:Nakagami noise m=0.7, Ω=0.1, e: Nakagami synthetic image with m=0.7, Ω=0.1, f: with m=0.3, Ω=0.1

3. RESULTS

3.1. Synthetic images

Synthetic images were generated for values of Ω from $10^{-4.5}$ to $10^{-1.5}$ and of *m* from 0.1 to 1.5. For each image, the parameters were estimated on 110 non-overlapping windows (2x2mm). Figs. 2 a.b.c show the mean error on the estimation of *m* for the MB (orange circle), ML (red square) and combined (blue triangle) methods, either for different values of Ω when *m* is fixed at 0.2 or 0.6, or for different values of m for Ω=0.001. The results of the first two methods using a linear scale for the discretization are also shown (corresponding colours and symbol, dashed line). For each combination of parameters, the method we propose performs better than the other ones, with a mean error smaller than 0.02, whilst the other methods show a mean error between 0.04 and 1.2. More importantly, the results of the combined method are constant for various values of Ω and fairly stable when *m* varies, whereas the performances of the two other methods vary considerably according to both Ω and *m*. This invariance is important. Specifically, while computing the Nakagami images on clinical data, a certain error could be acceptable, as soon as it is limited and stable. Interestingly, the mean error obtained with our technique is lower than the best of either the other ones. This can be explained as the best estimation is chosen for each single windows. Though the use of a logarithmic scale does not make any difference for the traditionnal estimator (the yellow plain and dash lines merge), it leads to significantly better performance of the ML estimator. Indeed, the ML estimator is more sensitive to changes of the smaller values as it considers the logarithm of the square of the signal, while the traditional approach uses the 4th power. Discretization error on the smaller intensity values are thus more likely to have an impact on the estimation.
Fig. 2.d shows the proportion of windows where the chosen parameter pair is the one estimated by the MB (red, dashed line) and ML based methods (blue, plain line) in the proposed framework, for two values of Ω and m varying.

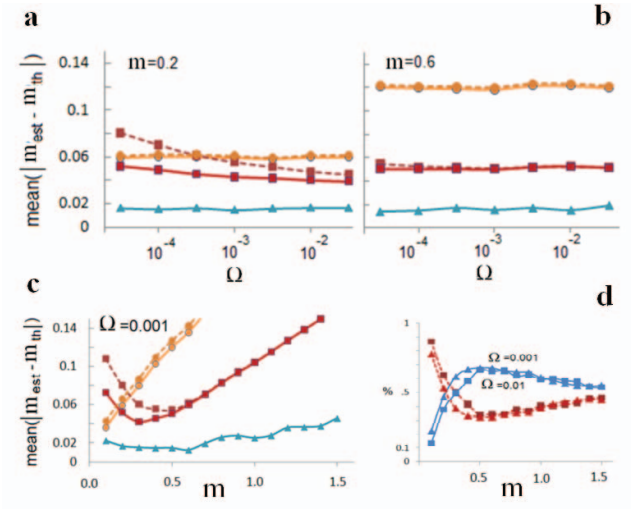


Figure 2: Evolution of the mean error of m for m=0.2(top left), m=0.6 (top right) and Ω=0.001 (bottom left) for different methods(cf. Text); and evolution with m of the proportions of estimations with the MB(red) and ML(blue) estimator for Ω=0.01 and Ω=0.001

3.2 Application to real images

The images used in this work are US breast images acquired with a Zonare Z.one with a L10-5 probe (128 elements) and a central frequency of ~7MHz. The envelope of the RF-data was computed by the Hilbert transform and the values were scaled between 0 and 1.
The new method was applied to 14 US breast images along with the ML and MB methods. Since we do not know the true Nakagami parameters, we propose to measure the benefits of using our technique by comparing the goodness of fitting between the observed and modelled distribution for our method and for the traditional one. With an average increase of 26% of the relative difference (Table 1), we can fairly assume that the fitting is substantially better when the parameters are estimated with our method. In addition, to justify the utilization of our technique and the additional - though small- complexity of its implementation, we also measured the pixel-by-pixel difference of the estimation of *m*. On average, the difference between the *m*-parametric images is 0.10. This difference is of the same order of difference between the average of *m* between 30 benign and 30 malignant breast tumour found in [3]. It is then fair to

consider it significant. Finally, the combination of two estimators would not be relevant if one of them was chosen largely more often than the other. To show that this is not the case, the proportion of points using the MB estimator was computed. With a 39%/61% repartition, it shows that the framework takes advantage of both methods (see also Fig. 3b).

Table 1

	Δd/d	*Δm*	*% time MB selected*
average	*26%*	*0.10*	*39%*

Average values of the relative difference of the goodness of fitting measure and of the estimated m parameter, and mean proportion of choice of the moment-based estimator.

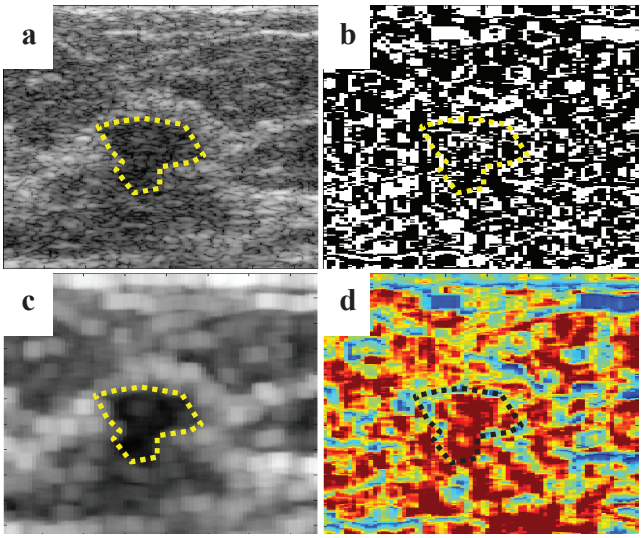


Figure 3. a: Example of US breast image; b: chosen estimator (white: ML, black : moment based); c: Ω map; d: m map (blue : 0 ; red : 2)

Figure 3.a. shows a region of interest of a US images of breast. A fibroadenoma can be observed in the center (yellow dots). Figure 3.c. and 3.d are the Nakagami maps of respectively the first and second parameter (Ω and *m*), and Fig. 3.b represents the points (in white) where the ML estimator has been chosen (the points in black representing the points where the moments-based estimator was chosen). This image presents clusters of white points, with no visible correlation with the mean intensity and the *m*-parametric image. This shows that both methods can be used for any value of Ω and *m*.

9. DISCUSSION - CONCLUSION

In this work, we have proposed a simple method to combine two estimators of the Nakagami parameters. As the two estimators have different behaviour over the ranges of parameters, computing both of them and chosing *a posteriori* the best ensures an increase in the accuracy of the estimation. Results on synthetic images showed a considerable decrease of the estimation error and better stability. The analysis of the results on breast images showed the advantages of using a combined approach and justified the required small additional computation time. However, it only consists in the computation in the sliding window of the term $E[ln(r^2)]$ and of the CDF of the observed and model distribution. By its simplicity, this framework could be used in any study using Nakagami imaging. At the same time, alternative estimators of the Nakagami parameters could easily be incorporated.

Furthermore, two additional ideas have been developed. The first is a method for synthesizing images presenting real speckle pattern with a given Nakagami distribution. Though we only considered uniform images, it should be possible to incorprorate geometrical or anatomical structures, thus providing a fast and easy way of creating test-images for image processing techniques. Finally, a map of the goodness of fitting between the observed distribution and the model can be built, as it is computed at each point, and could be considered as a measure of the confidence one could have in the estimated parameters at each point. This could be included for example as a weighting parameters while averaging the Nakagami parameters for a whole manually-segmented tumor, thus decreasing the impact of the bad estimations occuring on the boundaries.

10. ACKNOLWEDGMENT

This work is funded by the EPSRC and the Wellcome Trust, grant n° WT 088877/z/09/z.

11. REFERENCES

[1] PM Shankar. “A general statistical model for ultrasonic backscattering from tissues”. *IEEE Trans Ultrason Ferroelec Freq Contr*; vol.47, pp.727–736, 2000

[2] PH Tsui, CC Chang. “Imaging local scatterer concentrations by the Nakagami statistical model”. *Ultrasound Med Biol* , vol.33, pp.608–619, 2007

[3] PH Tsui et al. “Classification of Benign and Malignant Breast Tumors by 2-D Analysis Based on Contour Description and Scatterer Characterization,”*IEEE Trans.Med. Imaging,* vol29, pp. 513-522, 2010.

[4] A Larrue, JA Noble, "Nakagami imaging with small windows," *IEEE International Symposium on Biomedical Imaging*, 2011

[5] PH Tsui, SH Wang, “The Effect of Transducer Caracteristics on the estimation of Nakagami parameter as a function of scatterer concentration”, *Ultrasound Med Biol* ;vol.30, pp.1345–1353, 2004

[6] J. Cheng, NC. Beaulieu, “Maximum-Likelihood based estimation of the Nakagami m parameter,” *IEEE Commun. Lett.*, vol.5, pp. 101-103, Mar. 2001

[7] P. Coupé et al, “ NonLocal Means-based Speckle Filtering for Ultrasound Images”, *IEEE Trans. Image Proc.*, vol. 18(10), pp.2221-2229, Oct. 2009.